Doubly radiative $\eta^{(\prime)}$ decays: interplay of vector, scalar, and tensor contributions

Rafel Escribano[1,2,*], *Sergi* Gonzàlez-Solís[3,4,**], and *Emilio* Royo[2,5,***]

[1]Grup de Física Teòrica, Departament de Física, Universitat Autònoma de Barcelona, 08193 Bellaterra (Barcelona), Spain
[2]Institut de Física d'Altes Energies (IFAE), The Barcelona Institute of Science and Technology, Campus UAB, 08193 Bellaterra (Barcelona), Spain
[3]Departament de Física Quàntica i Astrofísica (FQA), Universitat de Barcelona (UB), c. Martí i Franquès, 1, 08028 Barcelona, Spain
[4]Institut de Ciències del Cosmos (ICCUB), Universitat de Barcelona (UB), c. Martí i Franquès, 1, 08028 Barcelona, Spain
[5]Departamento de Matemáticas, Física y Ciencias Tecnológicas, Universidad Cardenal Herrera-CEU, CEU Universities, 46115 Alfara del Patriarca, València, Spain

Abstract. The doubly radiative decays $\eta^{(\prime)} \to \pi^0(\eta)\gamma\gamma$ probe the interplay of vector-, scalar-, and tensor-meson exchanges beyond leading-order Chiral Perturbation Theory. We summarise a theoretical description combining Vector Meson Dominance, the Linear Sigma Model, and, for $\eta^{(\prime)} \to \pi^0\gamma\gamma$, a chiral-inspired $a_2(1320)$ tensor-meson exchange. Although vector-meson exchanges dominate, the destructive vector–tensor interference amounts to about 18% of the $\eta \to \pi^0\gamma\gamma$ signal and significantly distorts the low-$m^2_{\gamma\gamma}$ spectrum. Our resulting prediction, $\mathrm{BR}(\eta \to \pi^0\gamma\gamma) = 1.17(17) \times 10^{-4}$, agrees well with the recent KLOE-2 measurement but lies about 5σ below the PDG average, while the $\eta' \to \pi^0(\eta)\gamma\gamma$ predictions are consistent with the BESIII data.

1 Introduction

The η and η' mesons are flavour-neutral pseudoscalars, eigenstates of C, P and G parity with all additive quantum numbers equal to zero, making them a remarkably clean laboratory in which to stress-test the Standard Model (SM) and search for physics beyond it, complementary to direct searches at the energy frontier [1]. Among the accessible channels, the doubly radiative decay $\eta \to \pi^0\gamma\gamma$ has attracted particular interest, as it constitutes a long-standing benchmark for low-energy QCD: the leading orders of Chiral Perturbation Theory (ChPT) either vanish or are strongly suppressed, shifting the dominant contributions to unusually high chiral orders that are more efficiently resummed in terms of meson-resonance exchange [2, 3]. Despite decades of effort, both the value of the decay width and its underlying dynamics remain controversial: measurements by GAMS-2000 [4], Crystal Ball [5] and A2 at MAMI [6] cluster around $\mathrm{BR} \sim (2.2\text{–}2.5) \times 10^{-4}$, whereas the recent KLOE-2 measurement finds a factor of roughly 2.6 lower value, $\mathrm{BR}(\eta \to \pi^0\gamma\gamma) = 0.98(11)(14) \times 10^{-4}$ [7].

*e-mail: rescriba@ifae.es
**e-mail: sergig@icc.ub.edu
***Speaker, e-mail: emilio.royocarratala@uchceu.es

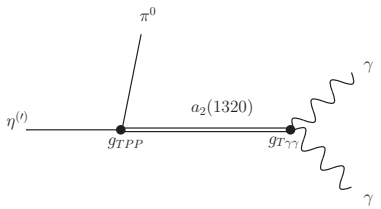


Figure 1. Schematic diagram for the a_2-exchange contribution to $\eta^{(\prime)} \to \pi^0\gamma\gamma$.

The sister processes $\eta' \to \pi^0\gamma\gamma$ and $\eta' \to \eta\gamma\gamma$ complement this picture and were measured for the first time by BESIII [8, 9]. In this contribution we summarize our theoretical description of the three decays, in which the vector- and scalar-meson exchange contributions are evaluated within Vector Meson Dominance (VMD) and the Linear Sigma Model (LσM), respectively [10], and, for $\eta^{(\prime)} \to \pi^0\gamma\gamma$, the $a_2(1320)$ tensor-meson exchange is additionally incorporated through a chiral-inspired formalism [11].

2 Theoretical framework

2.1 Vector- and scalar-meson exchanges

The vector-meson contributions proceed through the decay sequence $\eta^{(\prime)} \to V\gamma$ followed by $V \to \pi^0(\eta)\gamma$, with six diagrams contributing to the amplitude, corresponding to the exchange of $V = \rho^0, \omega, \phi$ in the t- and u-channels. Combining the $VP\gamma$ vertices with the propagator of the exchanged resonance, one arrives at the VMD amplitude

$$\mathcal{A}^{\text{VMD}}_{\eta\to\pi^0\gamma\gamma} = \sum_{V=\rho^0,\omega,\phi} g_{V\eta\gamma} g_{V\pi^0\gamma} \left[\frac{(P\cdot q_2 - m_\eta^2)\{a\} - \{b\}}{D_V(t)} + \left\{ \begin{array}{c} q_2 \leftrightarrow q_1 \\ t \leftrightarrow u \end{array} \right\} \right], \tag{1}$$

where $t, u = m_\eta^2 - 2P\cdot q_{2,1}$ are Mandelstam variables, P is the four-momentum of the decaying meson, $\epsilon_{1,2}$ and $q_{1,2}$ the polarization and four-momentum vectors of the photons, and

$$\begin{aligned} \{a\} &= (\epsilon_1\cdot\epsilon_2)(q_1\cdot q_2) - (\epsilon_1\cdot q_2)(\epsilon_2\cdot q_1)\,, \\ \{b\} &= (\epsilon_1\cdot q_2)(\epsilon_2\cdot P)(P\cdot q_1) + (\epsilon_2\cdot q_1)(\epsilon_1\cdot P)(P\cdot q_2) \\ &\quad - (\epsilon_1\cdot\epsilon_2)(P\cdot q_1)(P\cdot q_2) - (\epsilon_1\cdot P)(\epsilon_2\cdot P)(q_1\cdot q_2)\,. \end{aligned} \tag{2}$$

The ρ^0 propagator uses an energy-dependent width to account for its sizeable decay width, whereas the ω and ϕ mesons use the usual Breit–Wigner propagator with constant width. The amplitudes for $\eta' \to \pi^0\gamma\gamma$ and $\eta' \to \eta\gamma\gamma$ follow the same structure with the appropriate replacements of masses and couplings. The $g_{VP\gamma}$ couplings are determined directly from the experimental $V(P) \to P(V)\gamma$ radiative widths [12], rendering the treatment of vector exchanges model independent. The scalar-meson contributions are evaluated within the LσM via kaon- and pion-loop diagrams complemented by s-channel exchange of the $a_0(980)$, $\sigma(500)$ and $f_0(980)$ resonances, using complete one-loop propagators, rather than simple Breit–Wigner forms, to correctly capture the near-threshold and broad character of these states. We refer the reader to Ref. [10] for the full expressions.

Table 1. Individual contributions and total prediction for the $\eta \to \pi^0\gamma\gamma$ decay width (upper part), compared with experimental measurements (lower part).

Term	Value (eV)
Vectors (V)	0.1661
Scalars (S)	0.0005
a_2	0.0020
V–S interference	0.0121
V–a_2 interference	−0.0270
Γ_{th}	0.1538
BR_{th}	$1.17(17) \times 10^{-4}$
BR_{exp} (PDG [12])	$2.55(22) \times 10^{-4}$
BR_{exp} (KLOE-2 [7])	$0.98(11)(14) \times 10^{-4}$

2.2 Tensor $a_2(1320)$ exchange

Motivated by the fact that scalar-meson exchanges have consistently been found to be subdominant and insufficient to explain the outstanding experimental discrepancies, and that the $a_2(1320)$ is prominently observed in the crossed channel $\gamma\gamma \to \pi^0\eta$ [13], we further incorporate the $a_2(1320)$-exchange contribution to $\eta \to \pi^0\gamma\gamma$, shown in Fig. 1, following the chiral tensor-meson formalism of Ref. [14]. The relevant Lagrangian coupling the tensor nonet $T_{\mu\nu}$ to two pseudo-Nambu–Goldstone bosons is

$$\mathcal{L}_{TPP} = g_{TPP}\langle T_{\mu\nu}\{u^\mu, u^\nu\}\rangle\,, \tag{3}$$

and an analogous $T\gamma\gamma$ coupling governs the $a_2 \to \gamma\gamma$ vertex [14]. Using the experimental branching ratios $\text{BR}(a_2 \to \pi\eta) = 14.5(1.2)\%$ and $\text{BR}(a_2 \to \gamma\gamma) = 9.4(7) \times 10^{-6}$ [12], one determines $|g_{TPP}| = 21.5(1.0)$ MeV and $|c_{T\gamma\gamma}| = 1.2 \times 10^{-4}$ MeV^{-1}. Combining these vertices with the standard spin-2 propagator and the energy-dependent width $\Gamma_{a_2}(s)$, summed over the $\rho\pi$, $\eta\pi$, $K\bar{K}$, $\gamma\gamma$ and $\omega\pi\pi$ channels [13], one obtains the tensor-exchange amplitude

$$\mathcal{A}^{a_2}_{\eta\to\pi^0\gamma\gamma} = \frac{32e^2}{3F_\pi^2} g_{TPP}\, c_{T\gamma\gamma} \cos\phi_P\, P^\mu p^\nu \frac{P_{\mu\nu,\rho\sigma}(s)}{m_{a_2}^2 - s - i m_{a_2}\Gamma_{a_2}(s)}$$
$$\times \Big\{ g^{\rho\alpha} q_1^\beta q_2^\sigma + g^{\sigma\beta} q_1^\rho q_2^\alpha - g^{\rho\alpha} g^{\sigma\beta}(q_1\cdot q_2) - g^{\alpha\beta} q_1^\rho q_2^\sigma + \frac{1}{2} g^{\rho\sigma}\big[g^{\alpha\beta}(q_1\cdot q_2) - q_1^\beta q_2^\alpha\big] \Big\} \epsilon^*_\alpha(q_1)\epsilon^*_\beta(q_2)\,, \tag{4}$$

where ϕ_P is the η–η' mixing angle, and the amplitude for $\eta' \to \pi^0\gamma\gamma$ follows with $m_\eta \to m_{\eta'}$ and $\cos\phi_P \to \sin\phi_P$. This amplitude is fully determined up to the overall sign of $g_{TPP}\, c_{T\gamma\gamma}$, which we fix by requiring an unambiguous description of the a_2 line shape in the $\gamma\gamma \to \pi^0\eta$ Belle data [13]; the positive sign is preferred and translates into a *destructive* interference with the vector-exchange amplitude in the decay region.

3 Results and discussion

The total amplitude for $\eta \to \pi^0\gamma\gamma$ is built as the coherent sum $\mathcal{A} = \mathcal{A}_{\text{VMD}} + \mathcal{A}_{\text{L}\sigma\text{M}} + \mathcal{A}_{a_2}$, and the individual contributions to the decay width are collected in Table 1. Vector-meson exchanges dominate with about 108% of the total signal, while the *destructive* vector–$a_2(1320)$ interference represents approximately 18% of the signal; the remaining pieces (V–S interference, standalone a_2, scalar exchange and the negligible scalar–tensor interference) all lie below 10%. This yields $\Gamma(\eta \to \pi^0\gamma\gamma) = 0.154(22)$ eV, i.e. $\text{BR}(\eta \to \pi^0\gamma\gamma) = 1.17(17) \times 10^{-4}$, about 14% smaller than our previous VMD+LσM-only prediction [10]. As shown in Fig. 2, this result is in excellent agreement with the recent KLOE-2 measurement (within

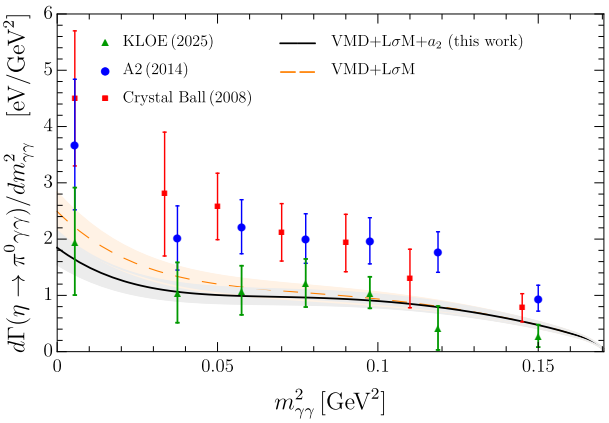


Figure 2. Comparison between the A2 [6], Crystal Ball [5] and KLOE-2 [7] measurements of the $\eta \to \pi^0\gamma\gamma$ invariant-mass distribution and our prediction (black solid), including vector, scalar and tensor exchanges. The orange dashed line omits the $a_2(1320)$ contribution [10].

0.8σ) but lies about 5σ below the PDG average [12]; the discrepancy between the black solid (with tensor) and orange dashed (without tensor) curves at low $m^2_{\gamma\gamma}$ illustrates how sizeable the vector–tensor interference is for the shape of the spectrum. In contrast, the $a_2(1320)$ plays essentially no role in $\eta' \to \pi^0\gamma\gamma$, which is overwhelmingly dominated by the exchange of an on-shell ω resonance: the pure VMD+LσM prediction, $\mathrm{BR}(\eta' \to \pi^0\gamma\gamma) = 2.82(20) \times 10^{-3}$, is reduced by only 1.4% once the tensor exchange is included, giving $2.78(21) \times 10^{-3}$, fully compatible with the BESIII measurement of $3.20(7)(23) \times 10^{-3}$ [8]. For $\eta' \to \eta\gamma\gamma$, where the a_2 exchange is phase-space suppressed and not yet included, vector-meson exchanges again dominate ($\sim$ 91%), but the scalar contribution is sizeable ($\sim$ 16%), with a destructive vector–scalar interference of about -7% that visibly shapes the spectrum; we obtain $\mathrm{BR}(\eta' \to \eta\gamma\gamma) = 1.17(8) \times 10^{-4}$ [10], consistent with BESIII, $8.25(3.41)(0.72) \times 10^{-5}$, and the upper limit 1.33×10^{-4} at 90% C.L. [9]. Both the experimental and theoretical situations for $\eta \to \pi^0\gamma\gamma$ remain inconclusive, motivating new measurements at JEF [15] and future dedicated η-factories such as REDTOP [16] and the planned facility at HIAF [17], as well as at a super-τ-charm facility [18]; the projected $\sim$ 5% precision of JEF after 100 days of beam time [1, 15] could distinguish the vector–tensor interference from a pure vector-exchange description.

4 Conclusions

We have presented a unified VMD+LσM+tensor description of the doubly radiative decays $\eta^{(\prime)} \to \pi^0\gamma\gamma$ and $\eta' \to \eta\gamma\gamma$. Although the standalone $a_2(1320)$ contribution to $\eta \to \pi^0\gamma\gamma$ is small, its destructive interference with the vector-meson resonances is significant ($\sim$ 18% of the signal) and reshapes the spectrum at low $m^2_{\gamma\gamma}$, bringing our prediction into excellent agreement with KLOE-2 while sharpening the tension with the PDG average and A2/Crystal Ball. The a_2 contribution is instead negligible in $\eta' \to \pi^0\gamma\gamma$, which remains dominated by the on-shell ω exchange, while scalar-meson exchanges, subdominant in both $\eta^{(\prime)} \to \pi^0\gamma\gamma$ channels, play a sizeable role in $\eta' \to \eta\gamma\gamma$; both predictions agree well with BESIII. The persistent spread among experimental measurements and theoretical predictions for $\Gamma(\eta \to \pi^0\gamma\gamma)$ calls for new precision measurements, particularly from JEF, to settle the KLOE-2/A2/Crystal Ball tension and test the destructive vector–tensor interference identified here.

References

[1] L. Gan, B. Kubis, E. Passemar, S. Tulin, Precision tests of fundamental physics with η and η' mesons, Phys. Rept. **945**, 1 (2022), 2007.00664. 10.1016/j.physrep.2021.11.001

[2] L. Ametller, J. Bijnens, A. Bramon, F. Cornet, Chiral perturbation theory for $\eta \to \pi^0\gamma\gamma$, Phys. Lett. B **276**, 185 (1992). 10.1016/0370-2693(92)90561-H

[3] P. Ko, $\eta \to \pi^0\gamma\gamma$ and $\gamma\gamma \to \pi^0\pi^0$ in $O(p^6)$ chiral perturbation theory, Phys. Lett. B **349**, 555 (1995), hep-ph/9503253. 10.1016/0370-2693(95)00284-R

[4] D. Alde et al. (Serpukhov-Brussels-Annecy(LAPP), Soviet-CERN), Neutral Decays of the η Meson, Z. Phys. C **25**, 225 (1984). 10.1007/BF01547921

[5] S. Prakhov et al., Measurement of the invariant-mass spectrum for the two photons from the $\eta \to \pi^0\gamma\gamma$ decay, Phys. Rev. C **78**, 015206 (2008). 10.1103/PhysRevC.78.015206

[6] B.M.K. Nefkens et al. (A2 at MAMI), New measurement of the rare decay $\eta \to \pi^0\gamma\gamma$ with the Crystal Ball/TAPS detectors at the Mainz Microtron, Phys. Rev. C **90**, 025206 (2014), 1405.4904. 10.1103/PhysRevC.90.025206

[7] D. Babusci et al. (KLOE-2), Measurement of $\eta \to \pi^0\gamma\gamma$ branching fraction with the KLOE detector (2025), 2505.09285.

[8] M. Ablikim et al. (BESIII), Observation of the doubly radiative decay $\eta' \to \gamma\gamma\pi^0$, Phys. Rev. D **96**, 012005 (2017), 1612.05721. 10.1103/PhysRevD.96.012005

[9] M. Ablikim et al. (BESIII), Search for the decay $\eta' \to \gamma\gamma\eta$, Phys. Rev. D **100**, 052015 (2019), 1906.10346. 10.1103/PhysRevD.100.052015

[10] R. Escribano, S. Gonzàlez-Solís, R. Jora, E. Royo, Theoretical analysis of the doubly radiative decays $\eta^{(\prime)} \to \pi^0\gamma\gamma$ and $\eta' \to \eta\gamma\gamma$, Phys. Rev. D **102**, 034026 (2020), 1812.08454. 10.1103/PhysRevD.102.034026

[11] R. Escribano, S. Gonzàlez-Solís, E. Royo, Assessment of the $a_2(1320)$ tensor-meson contribution to $\eta/\eta' \to \pi^0\gamma\gamma$ decays, Phys. Rev. D **112**, 114009 (2025), 2510.00787. 10.1103/y661-zt9k

[12] F. Takahashi et al. (Particle Data Group), Review of Particle Physics, Int. J. Mod. Phys. A **41**, 2630011 (2026). 10.1142/S0217751X26300115

[13] S. Uehara et al. (Belle), High-statistics study of $\eta\pi^0$ production in two-photon collisions, Phys. Rev. D **80**, 032001 (2009), 0906.1464. 10.1103/PhysRevD.80.032001

[14] G. Ecker, C. Zauner, Tensor meson exchange at low energies, Eur. Phys. J. C **52**, 315 (2007), 0705.0624. 10.1140/epjc/s10052-007-0372-x

[15] The JLab Eta Factory (JEF) Experiment, Update to the JEF proposal (PR12-14-004), https://www.jlab.org/exp_prog/proposals/17/C12-14-004.pdf

[16] J. Elam et al. (REDTOP), The REDTOP experiment: Rare η/η' Decays To Probe New Physics (2022), 2203.07651.

[17] X. Chen et al., Plan for a super η factory at Huizhou accelerator complex, Nucl. Sci. Tech. **36**, 137 (2025), 2407.00874. 10.1007/s41365-025-01708-1

[18] M. Achasov et al., STCF conceptual design report (Volume 1): Physics & detector, Front. Phys. (Beijing) **19**, 14701 (2024), 2303.15790. 10.1007/s11467-023-1333-z